THE ASTROPHYSICAL JOURNAL, 226:829–838, 1978 December 15

ICE MANTLES AND ABNORMAL EXTINCTION IN THE RHO OPHIUCHI CLOUD

D. H. HARRIS,* N. J. WOOLF,† AND G. H. RIEKE‡
Received 1977 December 1; accepted 1978 March 5

ABSTRACT

Results from a study of interstellar ice extinction in the ρ Oph dark cloud include measures of the 3.07 μm absorption band in the spectra of heavily obscured stars. These measures show that the abnormal extinction within the cloud does not result from the growth of ice mantles; mantles form only in the densest regions and are not accompanied by any significant change in the broad-band extinction law.

Subject headings: interstellar: abundances — interstellar: matter — nebulae: individual

I. INTRODUCTION

The abnormally high values of $R(\equiv A_V/E_{BV})$ and the large λ_{max} of polarization found in certain dense interstellar clouds, most notably the very dense cloud south of ρ Oph (Carrasco, Strom, and Strom 1973; Strom, Strom, and Carrasco 1974; Strom *et al.* 1975; Vrba *et al.* 1975; Grasdalen *et al.* 1975), may indicate the presence of larger than normal particles and the action of grain growth. The reduced relative strength of the interstellar diffuse bands may be a similar indication (Snow and Cohen 1974).

Using multiband photometry, we have examined the role of water ice as a grain growth material (e.g., Greenberg 1968). Analysis of the photometry establishes the shape of the infrared extinction curve, an indication of the grain size, and the absorption strength of the water-ice OH stretch band at 3.1 μm. We have found a relation between the relative ice abundance and the density of interstellar matter, a relation which significantly extends the conclusions of previous studies (Knacke, Cudaback, and Gaustad 1969; Merrill and Soifer 1974; Gillett *et al.* 1975; Merrill, Russell, and Soifer 1976), but which does not explain the abnormal extinction in the cloud.

II. OBSERVATIONS

Our observations were made using conventional infrared measurement techniques with the 1.5 m and 2.3 m telescopes of the University of Arizona, during the springs of 1975 and 1976. Table 1 lists the center wavelengths and FWHM values of the filter passbands.

Table 2 lists the magnitudes of the standard and comparison stars. The zero point of the magnitude system is set by the standard stars α Boo, α Vir, α Lyr, and β Lib (Johnson *et al.* 1966). The weakly reddened stars δ Sco and 22 Sco are secondary standards and principal comparison stars for the Ophiuchus region. Each was measured with high precision ($\sigma = 0.01$ mag) on three nights with full atmospheric extinction transforms, their colors having been determined using the optical region photometry and spectral types from Garrison (1967), our infrared photometry, and a model extinction curve.

Table 3 presents the infrared photometry of our program stars out to 3.8 μm. The $(K - \lambda)$ colors are from measures relative to comparison stars at nearly equal air mass. Measures of the stars VI Cyg 12 (Cyg OB 2 No. 12) and HD 168607 were made in order to

TABLE 1
FILTER CHARACTERISTICS

Name	log λ_0	λ_0 (μm)	FWHM (μm)
J..........	0.097	1.25	0.2
H..........	0.204	1.60	0.4
2.17........	0.3355	2.165	0.18
K..........	0.342	2.20	0.60
2.3..........	0.3701	2.345	0.06
3.0..........	0.4790	3.013	0.08
3.1..........	0.4925	3.108	0.07
3.4..........	0.534	3.420	0.16
L..........	0.554	3.58	1.01
3.8..........	0.582	3.82	0.51

TABLE 2
MAGNITUDES OF STANDARD AND COMPARISON STARS

Star Name*	*J*	*H*	*K*	*L*
α Boo[1]........	...	...	−3.00	−3.14
α Vir[1]........	...	...	+1.68	+1.67
α Lyr[2]........	...	...	+0.02	−0.02
β Lib[2]........	...	...	+2.86	...
δ Sco[2]........	2.58	2.61	+2.71	+2.66
22 Sco[2].......	5.04	5.08	+5.15	+5.10
BS 7769[3]......	...	...	+5.49	...
BS 7826[3]......	...	...	+5.42	...
BS 8677[3]......	...	...	+6.19	...

* Code indicates the type of usage of the star. (1) Stars are absolute standards used only to set the zero point of the magnitude system; (2) stars are used both as zero-point standards and color-difference comparison stars; (3) stars are used for color comparison only. (Magnitudes of code 3 stars are our measures.)

* Project Starlight, Int.

† Steward Observatory, University of Arizona.

‡ Steward Observatory and Lunar and Planetary Laboratory, University of Arizona, Alfred P. Sloan Fellow.

1978ApJ...226..829H

TABLE 3

MAGNITUDES OF PROGRAM STARS

NAME	FILTER										REF.
	J	H	2.165	K	2.345	3.013	3.108	3.42	L*	3.82	
Ophiuchus Region											
HD 147889.....	5.301	4.856	4.582	4.564 ± 0.013	4.523	4.421	4.416	4.335	4.301 ± 0.05	4.288	1
	...	...	...	4.60 ± 0.05	...	...	...	...	4.42	...	2
	5.28	4.80	...	4.52	...	...	...	...	4.38	...	3
SR 3†.........	7.679	6.970	6.536	6.491 ± 0.006	6.438	6.232	6.202	6.107	6.067	5.977	1
	...	...	...	6.47 ± 0.05	...	...	...	...	6.41 ± 0.05	...	2
GS 31‡§.......	8.920 ± 0.12	7.404 ± 0.10	6.750	6.683 ± 0.010	6.537	5.868	5.801	5.507	5.365	5.213	1
	8.883	7.380	...	6.566 ± 0.08	...	...	...	...	5.56 ± 0.15	...	4
	11.42	9.35	...	7.26	...	...	...	...	5.73	...	5
GS 32‡§.......	10.892	8.502	7.131	7.053 ± 0.014	6.838	6.034	5.885	5.535	5.321	...	1
	>11.47	8.15	...	6.64	...	...	...	...	4.93	...	5
GS 26‡§.......	14.04 ± 0.13	11.136	...	8.984 ± 0.02	8.690	7.790 ± 0.05	...	7.10	(6.89)	...	1
	≥12.08	10.55	...	8.88	...	...	...	...	6.88	...	5
VS 18§.........	15.19 ± 0.30	12.19 ± 0.04	...	9.79 ± 0.02	9.502 ± 0.02	9.375 ± 0.04	...	8.05 ± 0.05	(7.90)	...	1
	≥13.17	10.27	...	8.91	...	...	...	...	...	...	5
GS 30‡§.......	14.56 ± 0.30	10.81	...	8.13 ± 0.02	7.87	7.41 ± 0.06	...	6.31	(6.12)	...	1
	11.48	8.84	...	7.74	...	...	...	...	6.73	...	5
VS 17§.........	15.69 ± 0.4	11.90 ± 0.03	8.955	8.845 ± 0.012	8.434	7.930	7.799	6.468	6.224	5.833	1
	...	11.33	...	8.54	...	...	...	...	6.64	...	5
VS 26§.........	...	15.04 ± 0.4	...	10.51 ± 0.02	...	11.39 ± 0.3	...	...	8.07 ± 0.03	...	1
	...	10.83	...	9.12	...	...	...	...	7.79	...	5
Other Program Stars											
HO 168607.....	...	...	3.403	3.345 ± 0.01	3.289	3.072	3.010	2.905	2.881	...	1
VI Cyg 12......	...	...	2.744	2.715 ± 0.02	2.635	2.405	2.375	2.281	2.217	2.178	1

* The numbers in parentheses are computed from the same polynomial fits (to our photometry, generally from 1.6 to 3.4 μm) which are used in computing the continuum level at the wavelength of the ice band.

† The designation SR 3 is from the slit spectrum survey of Struve and Rudkjobing 1949. This designation is used in the 2 μm survey paper of Grasdalen *et al.* 1975, and by Carrasco *et al.* 1973 and Vrba *et al.* 1975.

‡ The GS numbers are entry numbers in the Table 1 of Grasdalen *et al.* 1975 where the source coordinates are specified.

§ The VS numbers specify sources in Table 1 of Vrba *et al.* 1975. The Vrba *et al.* photometry of GS 26, GS 30, GS 31, and GS 32 is according to their Table 2. However, comparing coordinates for those GS sources with VS designations reveals several designation errors, bringing into question the identifications of the VS sources and perhaps partially explaining the discrepancies with our photometry.

REFERENCES.—(1) D. H. Harris and G. Rieke for the present work; (2) Carrasco *et al.* 1973; (3) van Breda *et al.* 1974; (4) Rydgren *et al.* 1976; (5) Vrba *et al.* 1975.

determine the ice band strength and extinction curve shape for stars obscured mostly by dust in the general interstellar medium. The scatter in our magnitude and color measures from night to night and between observers was within the expected range of photometric uncertainty and gave no indication of stellar variability; therefore, the tabulated measures are weighted means. In the wavelength interval 2.1 to 3.8 μm the accuracies of the color measures are generally much better than the tabulated K magnitude uncertainties. The non-statistical uncertainties in color are generally about 0.01 mag for the brighter sources, increasing to 0.03 mag for the faintest sources. Statistical errors are given whenever they exceed a few percent. All the tabulated magnitudes are effectively monochromatic, having been corrected for filter width effects using the formulae of King (1952). The tabulated magnitudes taken from other authors include similar corrections, making them directly comparable with ours.

Our observations of sources in the Ophiuchus region agree reasonably well with those of Rydgren, Strom, and Strom (1976), Carrasco, Strom, and Strom (1973), Johnson *et al.* (1966), and van Breda, Glass, and Whittet (1974). Our measures of VI Cyg 12 agree with previous values given by Voelcker (1975) and Gillett *et al.* (1975). However, comparing our measures with those of Vrba *et al.* (1975) reveals discrepancies of more than a magnitude in several instances. We have no explanation for these discrepancies, but we wish to emphasize that the repeatability and signal-to-noise ratio of our measurements indicate errors of no more than a few percent (except where larger errors are indicated in Table 3).

III. DISCUSSION

a) *Color Excess Ratios*

Table 4 lists the available optical-region photometry, spectral types, color excesses, and excess ratios for sources we have measured. There is some uncertainty in the spectral types and therefore the intrinsic colors of these stars, particularly VI Cyg 12 (Chaldu, Honeycutt, and Penston 1973) and SR 3 (discussed below). However, the spectral type uncertainties should not seriously affect the computed excess ratios, uncertainty of intrinsic color being the major source of error. Total uncertainties in the excess ratios are generally between 2% and 6%. The values of R are extrapolations using extinction curves (Fig. 1 and Harris 1976). It is noteworthy that in Table 4 the values of R for the two visible stars in Ophiuchus are nearly equal at $R = 4.3$, in agreement with the analyses by Whittet (1974) and Carrasco, Strom, and Strom (1973).

The assembly of sources in the Ophiuchus cloud resembles a newly formed open cluster still embedded in the dense, cold gas and dust from which it formed (Carrasco, Strom, and Strom 1973; Harris 1976). It seems reasonable that the IR sources are heavily obscured early-type stars. Therefore, our initial IR color-excess ratios were computed assuming that all the sources are A0 V type stars (fortunately, these ratios are not sensitive to the exact spectral type chosen). The similarity of the resulting IR extinction curves (see Table 5 and Fig. 1) supports the contention that the sources are heavily obscured stars. With all the sources at the distance modulus of the association, $(m - M) = 6.0$ (Jones 1970; Walborn 1972; Whittet 1974), their absolute magnitudes range between about -3 and $+1$, showing that they are most likely either B or A dwarfs; G, K, or M giants; or luminosity class II stars (Blaauw 1963).

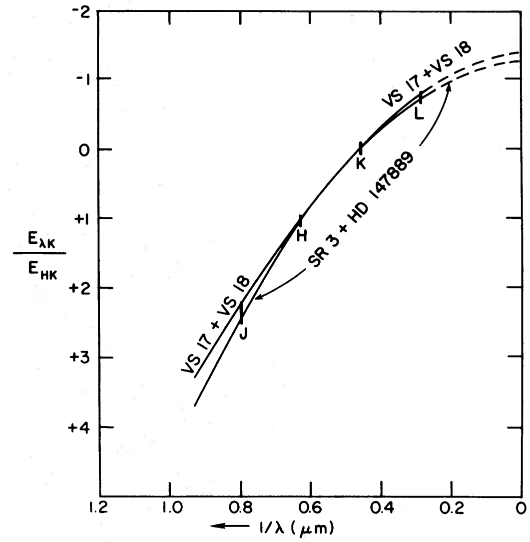

FIG. 1.—The mean Ophiuchus extinction curves in the infrared. Measurements of the moderately obscured sources SR 3 and HD 147889 have been averaged and normalized to $E_{HK} = 1$ for comparison with measurements of the heavily obscured sources VS 17 and VS 18, similarly averaged and normalized.

The normal spectral type–absolute magnitude diagram of a young open cluster shows that most of the stars with $1 \geq M_v \geq -3$ are on the main sequence and a few are giants; it is extremely rare to find a luminosity class II star. The gas within the cloud is mostly cold ($T_g \approx 20$ K) and neutral, with $(n_e/n) \approx 10^{-5}$ except in a few compact regions around embedded hot stars (Brown *et al.* 1974), while Fazio *et al.* (1976) find that the dust grain temperature, $T_d \approx 50$ K, is consistent with heating by the recognized embedded stars. These observations show that none of the stars in this region is earlier than late O spectral type and that the embedded stars are most likely between B2 V and B8 V spectral type. Our filter set includes a narrow filter within the 2.31 μm CO band which should permit us to identify red giant stars (Frogel *et al.* 1975). Our measures give no indication of CO absorption in any of the measured IR stars (see Table 5). These arguments all indicate that the IR stars are B or A dwarf stars.

With the IR sources tentatively classified, we estimated their spectral types from their computed absolute magnitudes (see Table 5), and used the intrinsic colors of the estimated spectral types to compute a revised set of color-excess ratios. For HD 147889 comparison with the known spectral type shows

TABLE 4*

COLOR EXCESSES OF STARS WITH OPTICAL PHOTOMETRY

Star Name	V	Sp	E_{BV}	E_{VH}/E_{BV}	E_{VH}/E_{BV}	E_{VK}/E_{BV}	E_{VL}/E_{BV}	R
HD 147889[a].....	7.90 ± 0.02[b]	B2 V[c]	1.09 ± 0.04[b]	2.88 ± 0.15	3.38 ± 0.17	3.72 ± 0.20	3.94 ± 0.20	4.13 ± 0.25
SR 3[d]...........	12.00[e]	B8 V[f]	1.42 ± 0.08[g]	3.17 ± 0.20	3.70 ± 0.25	4.07 ± 0.30	4.35 ± 0.30	4.51 ± 0.35
HD 168607[h].....	8.29[i]	B9 Ia$^+$p[i]	1.60 ± 0.03[i]	(2.42)[j]	(2.77)[j]	3.07 ± 0.12	3.35 ± 0.13	3.53 ± 0.15
VI Cyg 12[k]......	11.48[l]	B8 Ia[l]	3.24 ± 0.03	2.19	2.53	2.72	2.86	2.98
van de Hulst 15...	...	...	...	2.29	2.58	2.82	2.99	3.14

* The IR color excesses are probably uncertain by ~0.1 mag because of uncertainties in spectral type and intrinsic colors.

NOTES.—(*a*) The IR photometry of HD 147889 is by Harris and Rieke for the present work. Photometry by Serkowski 1968 and van Breda *et al.* 1974 generally agrees with ours within their given error estimates. (*b*) The V magnitude and E_{BV} of HD 147889 are weighted mean values from the literature. (*c*) The spectral type of HD 147889 is uniformly described as B2 V by Hiltner 1956, Garrison 1967, and recent works which may rely on the Hiltner and Garrison types. (*d*) The IR photometry of SR 3 is by Harris and Rieke for the present work. (*e*) The V magnitude of SR 3 is from Carrasco *et al.* 1973. (*f*) The spectral type is an average of the value given by Struve and Rudkjobing 1949 and our estimate from the star's absolute magnitude. (*g*) The E_{BV} of SR 3 uses the $(B - V)$ color of Carrasco *et al.* 1973, the spectral type from column (3), and the intrinsic colors from Johnson 1968. (*h*) The IR photometry of HD 168607 is by Harris and Rieke for the present work. (*i*) The optical photometry and spectral type of HD 168607 are from Hiltner 1956. (*j*) For HD 168607, the J and H excess ratios are obtained by interpolation and consequently are given in parentheses. (*k*) For VI Cyg 12 (Cyg OB 2 No. 12) the R, J, and H photometry are weighted means from values given in Voelcker 1975, and the K and L photometry is from the present work. (*l*) The optical photometry and spectral type of VI Cyg 12 are from Johnson 1968.

TABLE 5

EXTINCTION AND COLOR EXCESS RATIOS

Name	Sp	E_{HK}	E_{VK}	A_V	E_{VK}/E_{HK}	E_{RK}/E_{HK}	E_{JK}/E_{HK}	E_{KL}/E_{HK}	ΔL* (mag)
HD 147889..........	B2 V	0.37	4.05	4.5	10.9	(8.1)	2.46 ± 0.20	0.62 ± 0.10	0.0 ± 0.1
SR 3...............	B8 V	0.52	5.75	6.4	11.1	(8.2)	2.40 ± 0.20	0.77 ± 0.10	0.0 ± 0.1
GS 31..............	B5 V	0.78	(10.8)	(11.8)	(13.9)	10.3 ± 0.5	3.01 ± 0.1	1.67 ± 0.1	0.7 ± 0.2
	[K5 III	0.49	(7.1)	(7.8)	(12.0)	8.9 ± 0.5	2.27 ± 0.1	2.49 ± 0.1	1.0 ± 0.2]
GS 32..............	B4 V	1.52	(16.0)	(18.0)	(10.5)	7.8 ± 0.5	2.61 ± 0.1	1.13 ± 0.1	0.6 ± 0.2
	[M0 III	1.28	(11.6)	(13.3)	(9.1)	7.0 ± 0.5	2.25 ± 0.1	1.47 ± 0.1	0.9 ± 0.2]
GS 26..............	B6 V	2.21	(23.4)	(26.3)	(10.6)	(7.8)	2.34 ± 0.12	0.94 ± 0.03	0.4 ± 0.2
VS 18..............	B8 V	2.44	(24.7)	(27.9)	(10.1)	(7.5)	2.24 ± 0.17	0.77 ± 0.03	0.0 ± 0.2
GS 30..............	B2 V	2.76	(30.0)	(33.5)	(10.9)	(8.0)	2.40 ± 0.15	0.72 ± 0.03	0.0 ± 0.2
VS 17..............	B3 V	3.13	(31.7)	(35.8)	(10.1)	(7.5)	2.24 ± 0.20	0.83 ± 0.02	0.3 ± 0.3
VS 26..............	B2 V	4.61	(48.0)	(53.9)	(10.4)	(7.7)	(2.30)	0.53 ± 0.10	0.0 ± 0.5
VI Cyg 12..........	B8 Ia	3.24	8.80	9.65	11.7	7.8	2.3	0.64	0.0 ± 0.3
HD 168607..........	B9 Ia$^+$p	0.49	4.91	5.65	(10)	(7.0)	(2.1)	(0.90)	0.1 ± 0.1
vdeH 15............	...	...	...	...	13	8.4	2.3	0.77	...

* Estimated circumstellar emission at L.

good agreement, giving confidence in the estimated spectral types. But for SR 3 the estimated spectral type is B6, whereas Struve and Rudkjobing (1949) give A0. Considering the expected bias in their classification due to low dispersion and strong reddening, we have computed the color excess assuming a B8 V spectral type.

Table 5 and Figure 1 present the measured color-excess ratios and average extinction curves normalized to $E_{HK} = 1$. The excess ratios were normalized to E_{HK} because it is accurately measured for all the Ophiuchus stars and should not be affected by circumstellar emission. Magnitudes at R of 14.3 ± 0.4 for GS 31 and 18.5 ± 0.5 for GS 32 were measured on the Palomar Observatory Sky Survey prints by comparison with a calibrated sequence of red-print magnitudes. All other magnitudes used in computing the color-excess ratios in Ophiuchus are taken from the measures listed in Tables 3 and 4. In order to estimate the other excesses for the heavily obscured stars, it was necessary to use average color-excess ratios. Since, for both HD 147889 and SR 3, our measures show that $E_{VK}/E_{RK} = 1.35$ (a value not far from the mean of VI Cyg 12 and HD 168607), we assumed this ratio is constant in the Ophiuchus region and applied it to computing E_{VK} for the other stars. To find E_{RK} for the more heavily obscured stars we used the relation $E_{RK}/E_{JK} = 3.35$, which seems to be a representative value for the Ophiuchus region and not far from that found elsewhere. For VS 26, which has no J measure, we assumed $E_{JK}/E_{HK} = 2.30$, the average value of the ratio for the other heavily obscured stars. The extinction beyond the K filter was estimated using the mean extrapolated extinction curve assuming $E_{K\infty} = 1.30E_{HK}$. The estimated circumstellar emission ΔL (mag) is obtained by assuming that normal extinction gives $E_{KL}/E_{HK} = 0.75$. Because of the crudeness of these estimates and the small variation in curve shape, we have plotted average extinction curves in Figure 1.

From Table 5 both GS 31 and GS 32 show peculiar red and infrared extinction curves if they are assumed to be early-type dwarf stars (type determined by absolute-magnitude fit). However, if instead one assumes that the extinction curve is nearly normal, and estimates the spectral type from the (J to K) colors which result when the mean Ophiuchus extinction is removed, one finds that these stars resemble subluminous K or M giants. Table 5 includes late-type models of these stars, although this classification is doubtful because of the lack of CO absorption in their spectra. Their position in the H-R diagram is suggestive of pre–main-sequence objects which would reach the ZAMS as F stars. This identification seems questionable, however, since the 10 μm magnitude of GS 31 indicates an emission excess more like that in keeping with the B5 V model (see Table 6).

b) *Extinction Curve Interpretations*

For the lightly obscured stars in the Ophiuchus cloud, Tables 4 and 5 show that the optical and near-IR slopes are larger than would be normal for the general interstellar extinction, and that there is an apparent increase in the ratio of total to selective extinction, R, with obscuration (see also Carrasco, Strom, and Strom 1973, Fig. 2). In the infrared, extinction commonly varies as $(1/\lambda)^4$, a recognized characteristic of small dielectric spheres. As shown in Figure 1, the strongly obscured Ophiuchus stars show a dependence closer to $1/\lambda$, suggesting either the admixture of small absorbing particles (radius $a \lesssim 0.1\ \mu$m) or larger than normal dielectric particles ($a \approx 0.5\ \mu$m). That is, the extinction curve looks like a composite of extinction by "normal" and IR particles. The Ophiuchus cloud shows a nearly uniform abnormal extinction regardless of obscuration (or ice band strength—see below).

If one assumes that the IR particles are dielectrics, then the published dielectric sphere grain models (Wickramasinghe 1973) yield estimated grain sizes by fitting the extinction curve. Taking the normal ratio of total to selective absorption, $R \approx 3.2$, and the normal visual-region extinction curve, e.g., an average of VI Cyg 12 and HD 168607, and fitting to the corresponding properties of the relative extinction efficiency curve, $Q_e[(a/\lambda\!\!\!{}^-), n] \equiv \sigma/\pi a^2$, where n is the refractive index and $\lambda\!\!\!{}^- = \lambda/2\pi$ is the reduced wavelength, shows that in the normal interstellar medium, generally $Q_e(\lambda = 0.55\ \mu\text{m}) \approx 2.6$, and the mean particle radius $\bar{a} \approx (0.11\ \mu\text{m})/(n - 1)$. This size is consistent with similar fits done by Greenberg (1968, p. 310) and by Spitzer (1968, p. 67). [In the moderately opaque portions of the Oph cloud, where $R \approx 5.0$, $Q_e(\lambda = 0.55\ \mu\text{m}) \approx 3.2$ and $\bar{a} \approx (0.13\ \mu\text{m})/(n - 1)$.] On examining the more general case of Q_e curve fitting for dielectric spheres, we find that for $6 \gtrsim R \gtrsim 2.8$, the variation in $Q_e(\lambda = 0.55\ \mu\text{m})$ with grain size very nearly (to $\sim 6\%$) compensates for the size dependence of the geometric cross section of a constant mass of grains. Fitting this

TABLE 6*

MAGNITUDES OF OPHIUCHUS STARS HAVING MID-INFRARED PHOTOMETRY

Name	K	L	5 μm	10 μm	10.4 μm	10.6 μm
GS 31	6.68 ± 0.01	5.37 ± 0.02	5.38 ± 0.15	3.05 ± 0.10	...	...
GS 30	8.13 ± 0.02	(6.25) ± 0.03	4.60 ± 0.10	...	1.67 ± 0.05	1.63 ± 0.05
VS 17	8.85 ± 0.01	6.22 ± 0.02	4.67 ± 0.06	...	3.69 ± 0.11	3.51 ± 0.05

* All K and L photometry is from Table 3. For GS 31 the mid-IR photometry is from Rydgren *et al.* 1976. The remainder of the mid-IR photometry is by Rieke (for the present work). Tabulated errors are statistical errors. The 5 μm and 10 μm measures of Rydgren *et al.* 1976 are with broad-band filters. The 10.4 μm and 10.6 μm filters are 1.3 μm and 5 μm wide, respectively. Only the K and L magnitudes are monochromatic. However, the filter width corrections are small compared to the mid-IR emission excesses.

general $Q_e[(a/\lambda), n]$ to the optical extinction in the less obscured regions of the cloud ($1 \gtrsim E_{HK} \gtrsim 0.3$ and $6 > R > 4$) yields a constant absolute efficiency,

$$\xi(\lambda = 0.55\ \mu\text{m}) \equiv \frac{\pi a^2 Q_e}{\frac{1}{3}(4\pi a^3)\rho}$$

$$= \frac{3Q_e}{4a\rho} \approx 1.8 \times 10^5 \left(\frac{n-1}{\rho}\right) \quad \text{cm}^2\ \text{g}^{-1}\,,$$

where ρ is the grain density (g cm^{-3}).

The heavily obscured Ophiuchus stars show nearly linear extinction curves over a factor of 2 range in $1/\lambda$ centered at $\sim 1.5\ \mu$m (when the emission excess at L is removed). The relative extinction efficiency $Q_e[(a/\lambda)(n-1)]$ for the general dielectric sphere is nearly linear over a range of 3 in $1/\lambda$ centered at $(a/\lambda)(n-1) \approx 1.1$. Using the monodisperse approximation (i.e., that all particles are the same size) and matching the Q_e curve to the linear IR extinction yields $2\pi a(n-1)/1.5 \approx 1.1$, or $a \approx (0.26\ \mu\text{m})/(n-1)$. For such grains $Q_e(\lambda = 0.55\ \mu\text{m}) \approx 2.8$, so $\xi(0.55\ \mu\text{m}) \approx 8.0 \times 10^4(n-1)/\rho$ cm^2 g^{-1}. The combined errors of observation and Q_e curve-fitting make the estimated particle radius uncertain by about 30%. The extinction efficiencies are uncertain by a similar amount. If the grain refractive index is constant in the cloud, then the dielectric model grain for the more heavily obscured regions is about 2.2 times the size of the dielectric model particle in the less opaque regions (volume ratio is ~ 10 to 1), suggesting the action of a grain growth process.

If the IR extinction particles are Rayleigh absorbing particles ($k \geq 0.2$, $m = n - ik$), then because of their $\sim 1/\lambda$ extinction dependence one can only set an upper limit on particle size. This limit is $(a/\lambda) \lesssim 1.05/|m-1|$. For extinction linear out to $(1/\lambda) \sim 0.9\ \mu\text{m}^{-1}$, then $a \lesssim (0.18/|m-1|)\ \mu$m.

c) *Ice Band Extinction Measures*

To estimate the response of our two ice filters to ice band extinction, we examined the published ice band profiles of astronomical sources and compared them with normalized response curves for the filters and laboratory spectral tracings of various substances (Harris 1976). From this comparison, we estimate that the filters should respond to 90 ± 6% of the peak ice band extinction and that their ice band sensitivities should be about equal. In discussing the band, $\Delta m(\lambda)$ (magnitude) is defined as the extinction in excess of the average adjacent continuum extinction. For VS 17, the most precisely measured source with strong ice band extinction, our measures show that

$$\Delta m(3.013)/\Delta m(3.108) = 0.965 \pm 0.016\,,$$

just as expected. Our measure of the BN point source in Orion further tests the filter system's sensitivity to ice band extinction. For BN, we find $\Delta m(3.07) = 1.20 \pm 0.08$, which is 0.77 ± 0.10 of the $\Delta m(3.07)$ in the spectrum of Gillett *et al.* (1975). Considering the overlap of our filter profile and their published band profile, a compromise estimated response is 85 ± 5% of the true $\Delta m(3.07)$. The appropriate correction is included in our tabulated ice measures.

The presence of a prominent broad band at 3.07 μm in little-reddened carbon stars such as SS Vir (Merrill and Stein 1976), and its tentative identification with C_2H_2 in the cool stellar atmosphere, puts the identification of the 3.07 μm band in some doubt. However, the absence of 2.3 μm CO absorption in the Ophiuchus IR stars as well as other arguments show that the sources in our sample are probably not carbon stars.

Table 7 presents the corrected ice band extinction measures. The continuum level at the position of the ice band is estimated from a series of polynomial fits to the other filter measures. The degrees of the polynomial fits are given, as are the ratios $\Delta m(3.07)/E_{HK}$ and $\Delta m(3.07)/A_V$. Much of the uncertainty in the values of $\Delta m(3.07)$ and the ice ratios is due to uncertainty in the continuum level set by the polynomial fits. Uncertainties in estimating A_V make $\Delta m(3.07)/E_{HK}$ the preferred measure of relative ice extinction. Figure 2 shows the remarkable variation of relative ice extinction with E_{HK}. For $E_{HK} \lesssim 2.2$ ($A_V \lesssim 25$) the stars show no significant ice band extinction (except for HD 147889 which may be anomalous), while for $E_{HK} \gtrsim 2.2$ all of the stars yet measured show strong ice bands. Observations of additional sources are needed to determine the abruptness of the onset of ice extinction near this critical density.

In the more opaque regions of the Ophiuchus cloud, both sources with, and the sources without, measurable ice band extinction have very similar, if not indistinguishable, IR extinction curves (Table 5 and Fig. 1). Consequently, the large values of R and λ_{max} of polarization within the cloud do not result from the growth of ice mantles.

d) *Density Dependence of Ice Extinction*

Since it appears that each Ophiuchus source is seen through just one dominant dust concentration (Harris 1976), the value of E_{HK} can be directly related to the space average dust density. The critical value of E_{HK} for the presence of ice is ~ 2.2 mag and the scale of the dust concentrations is ~ 0.4 pc, indicating an approximate critical density of 5 mag pc^{-1} in E_{HK}. The large value of the critical density means that if the ice strength–density relation is generally applicable, then one should expect to find measurable ice only in the densest regions (where microwave studies indicate a gas density $n \approx 10^5$ cm^3).

The relation between ice abundance and dust density may be generally applicable. The apparent absence of ice band extinction along the generally low-density path toward the galactic nucleus (Soifer, Russell, and Merrill 1976), which has an $E_{HK} \approx 1.9$ (Becklin and Neugebauer 1968), is consistent with this concept.

The extinction for both HD 168607 and VI Cyg 12 is well below that needed to give the critical density (even if all the extinction were concentrated in a 1 pc cloud). From Table 7, we find no significant ice opacity for these stars (see also Gillett *et al.* 1975). Grasdalen

TABLE 7*

ICE BAND EXTINCTION MEASURES

Name	O.P.†	$\Delta m(3.07)$	E_{HK}	$\Delta m(3.07)/E_{HK}$	$\Delta m(3.07)/A_V$
HD 147889	1, 2, 3	0.040 ± 0.011	0.37	0.107 ± 0.030	0.0088 ± 0.0025
SR 3	1, 3	0.008 ± 0.010	0.52	0.017 ± 0.020	0.0013 ± 0.0015
GS 31	1, 2, 3	0.032 ± 0.015	0.78	0.042 ± 0.020	0.0027 ± 0.0015
GS 32	1, 2, 3	0.028 ± 0.030	1.52	0.018 ± 0.020	0.0016 ± 0.0020
GS 26	1, 3	0.175 ± 0.060	2.21	0.079 ± 0.030	0.0067 ± 0.0025
VS 18	1, 2, 3	1.05 ± 0.10	2.44	0.429 ± 0.040	0.038 ± 0.0035
GS 30	1, 3	0.694 ± 0.07	2.76	0.251 ± 0.025	0.021 ± 0.002
VS 17	1, 2	1.05 ± 0.10	3.13	0.336 ± 0.035	0.029 ± 0.003
VS 26	1, 2	3.1 ± 0.5	4.61	0.670 ± 0.11	0.058 ± 0.015
HD 168607	1, 2	0.033 ± 0.030	0.49	0.068 ± 0.061	0.0059 ± 0.0053
VI Cyg 12	1, 2	0.025 ± 0.015	0.61	0.041 ± 0.025	0.0026 ± 0.0016
NGC 2024:‡					
No. 1	...	0.0 ± 0.04	0.63	0.0 ± 0.06	0.000 ± 0.005
No. 2	...	1.3 ± 0.1	2.87	0.45 ± 0.05	0.041 ± 0.005
BN§	...	1.57 ± 0.04	4.4	0.36 ± 0.04	0.03 ± 0.01
Galactic‖ center (2 μm)	...	0.0 ± 0.1	1.7	0.0 ± 0.06	0.0 ± 0.01

* All measures of obscuration are in magnitudes.

† O.P. is the order of the polynomial used in estimating the continuum level at 3.07 μm.

‡ For NGC 2024 No. 1 and No. 2, $\Delta m(3.07)$ is from Merrill *et al.* 1976 and E_{HK} and A_V are from Grasdalen 1974.

§ For BN the value of $\Delta m(3.07)$ is from Gillett *et al.* 1975 and Merrill *et al.* 1976, E_{HK} is from photometry by Rieke for the present study, and A_V is from Grasdalen 1974.

‖ For the Galactic center 2 μm source the $\Delta m(3.07)$ is estimated using data in Soifer *et al.* 1976 and E_{HK} is estimated using data from Becklin and Neugebauer 1968 and from Soifer.

(1974) has discussed two IR stars in NGC 2024 where the estimated cloud scale is the 0.20 pc radius of the visible dust concentration (a radius like that of the H I cloud). The corresponding densities in E_{HK} are ~ 3.2 and 15 mag pc^{-1} for NGC 2024 No. 1 and No. 2, respectively. As predicted by the relation found in the Ophiuchus cloud, Grasdalen's measures show that No. 1 has no notable ice band extinction while No. 2 has strong ice band extinction (see also Merrill, Russell, and Soifer 1976). A similar argument can be made for the BN point source (see also Gillett *et al.* 1975), where the density is ~ 7 mag pc^{-1} in E_{HK} (cloud scale from Wilson, Jefferts, and Penzias 1970) and ice is detected. Strom, Strom, and Vrba (1976) and Strom, Vrba, and Strom (1976) have reported ice band extinction measures for sources in dark clouds. Although these measures are of low statistical weight, they are generally consistent with our derived relation for the Ophiuchus cloud.

e) Estimated Ice Fraction

In order to use the measured values of $\Delta m(3.07)$ to estimate the ice mass fraction we need an estimate of the absolute ice band extinction efficiency ($cm^2\ g^{-1}$) and a model of the wavelength-dependent absolute extinction efficiency of the assemblage of cloud particles.

A comparison of the values given by Sill (1976), Schaaf and Williams (1973), and Bertie, Labbé, and Whalley (1969) with the compilation of data in Irvine and Pollack (1968) shows a factor of 2 uncertainty in the absorption index k for ice. A representative refractive index at the band opacity maximum is $m \approx 1.20-0.64i$, with negligible opacity in the adjacent continuum. As will be shown later, the Rayleigh approximation gives an adequate estimate of the ice band extinction, thus $[\Delta\tau(3.07)/V] \approx 2.4 \times 10^4\ (cm^{-1})$, where V is the volume of material per unit area integrated along the line of sight. If $\rho_{ice} = 1\ g\ cm^{-3}$ for grains in interstellar conditions, then $\Delta\xi(3.07) = \Delta\tau(3.07)/\rho V \approx 2.4 \times 10^4\ cm^2\ g^{-1}$.

Assuming no major deviation from normal cosmic abundances (Allen 1964), we computed a series of grain models having the various compositions often put forth in the literature (e.g., silicates, graphite, etc.). The composition models were tested by comparing them with the Ophiuchus extinction observations scaled to the estimated H_2 density ($n \approx 10^5\ cm^{-3}$) and an assumed cloud dimension of ~ 0.4 pc. Within the errors of the model, all of the commonly proposed grain compositions are readily fitted to the Ophiuchus extinction observations by picking an appropriate grain size. This shows that the problem of particle size distribution cannot be separated from that of grain composition (exotic model particles such as nonvolatile hydrocarbons are the exception; they do not seem to be abundant enough). Since the available observations cannot be used to give an unambiguous grain composition, theoretical argument is necessary.

Since it is likely that most interstellar matter has been processed through dense clouds at least once during the life of the Galaxy (Shu 1975; Appenzeller 1975), the distinctive IR extinction particles could be important contributors to the general interstellar extinction. Thus the seemingly well-established dielectric nature of the normal interstellar particles (Martin, Illing, and Angel 1972; Zellner 1973; and references therein) argues against the significant presence of absorbing grains in dark clouds. Furthermore, if the

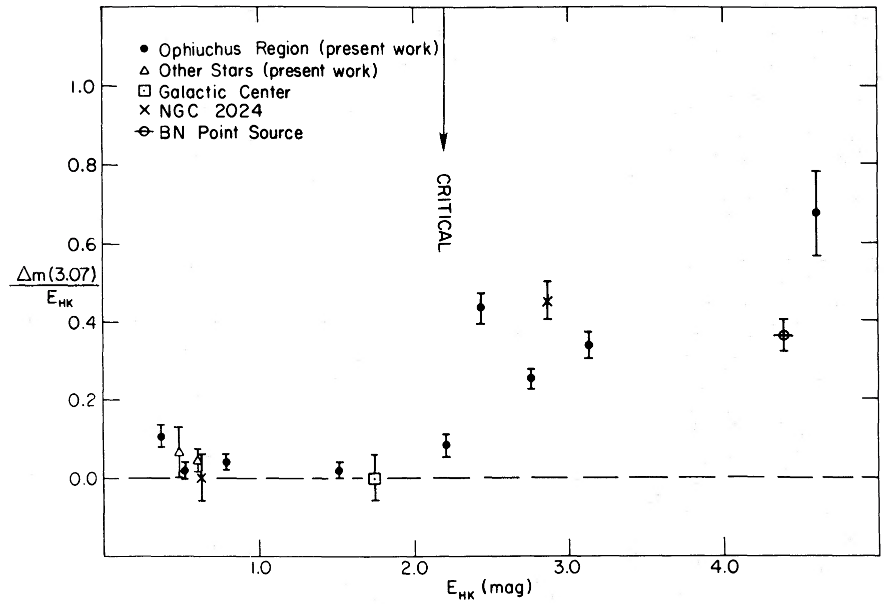

FIG. 2.—Dependence of relative ice extinction on E_{HK}. Measurements of the galactic center are from Soifer, Russell, and Merrill (1976), those of NGC 2024 are from Grasdalen (1974), and those of BN are from Gillett *et al.* (1975).

IR extinction grains are large dielectrics, grain destruction by collision (which probably increases with grain size, e.g., $-dN/dt \propto a^2$ [Greenberg 1966]) may act on the grains, yielding small particles which contribute to the pool of general interstellar-medium dust.

It is likely that grain growth within the Ophiuchus cloud is by coating, since below a gas temperature of about 100 K all metal atoms stick to the grains, and in the presence of oxygen the result is substances composed of oxides like SiO_2, Al_2O_3, etc. (Watson and Salpeter 1972; Aannestad 1973). Growth by coating is also suggested by the substantial reduction in the abundances of Si, Fe, and Mg in the dense gas of the cloud, presumably due to depletion onto the grains (Knapp, Kuiper, and Brown 1976). In addition, recent work on the fragmentation of particles during collisions (Hartmann 1976; Greenberg *et al.* 1977) indicates that fragmentation is more likely than coagulation if the grains are at high enough velocities for a significant number of collisions to occur during the life of the cloud (Harris 1976).

We have therefore assumed that silicates in combination with metal oxides are the principal grain constituents, with perhaps small quantities of graphite and carbon compounds, and with some ice in the heavily obscured regions. The model assumes that Si, Mg, Al, Fe, Ca, etc. are in combination with oxygen in the oxidation states found in chondrites (Wood 1975), and that most of the carbon is in CO. The silicate–metal oxide model matches the above-mentioned expectation of dominance by refractory dielectric particles. By direct comparison the model shows that (for $n_{H_2} = 10^5$ cm^{-3} over a path of $\sim$0.4 pc) there is approximately the correct amount of material to fit the measured extinction. For an average silicate–metal oxide material a reasonable complex refractive index is $m \approx 1.55 + 0.01i$, and a reasonable density is $\sim$3 g cm^{-3}, for both the large and small grains. To estimate the maximum available ice abundance we computed the ratio $(\bar{\rho}_{ice}/\bar{\rho}_{sil})$, the space-averaged density ratio of ice to silicates and metal oxides (assuming that all the oxygen not bound in CO, silicates, or metal oxides is in the form of ice). The resulting maximum $(\bar{\rho}_{ice}/\bar{\rho}_{sil})$ is $\sim$0.7.

We have approximated the grain size distribution by using two distinctive sizes: small grains [with $a = 0.12/(n-1) \approx 0.23$ μm] and large IR grains [with $a = 0.26/(n-1) \approx 0.48$ μm]. The size distribution then reduces to a single number, the ratio of the number densities of the two grain sizes averaged over the volume along the line of sight.

To estimate the number density ratio requires at least two observable extinction values whose ratio is sensitive to grain size. The ratio (A_V/E_{HK}) seems most suitable for this purpose because A_V is relatively insensitive to grain size for $a \gtrsim 0.15/(n-1)$ while E_{HK} is large for the IR grains and small for the small grains. Using the extinction efficiency values from Wickramasinghe (1973) and a refractive index, $m = 1.55 - 0.01i$, we have evaluated the expression

$$\frac{A_V}{E_{HK}} \approx \frac{\int \pi a^2 Q_e(0.55) n_g(a) da}{\int \pi a^2 [Q_e(1.6) - Q_e(2.2)] n_g(a) da} = f\left(\frac{N_s}{N_{IR}}\right),$$

where N_s and N_{IR} are the number densities (cm^{-2}) of small and IR particles, respectively. For the stars showing the distinctive IR extinction, $A_V/E_{HK} \approx 11.6$ and (N_s/N_{IR}) is $\sim$25. The number ratio is linearly dependent on A_V/E_{HK}, showing that an error in estimating A_V should not grossly affect the computed number ratio. The ratio is also insensitive to small variations in m and a. Using this ratio and the tabulated extinction efficiencies we computed the $(H - K)$ absolute extinction efficiency of the model grains, $\Delta\xi_{\rm sil} = \xi(1.6) - \xi(2.2)$,

$$\Delta\xi_{\rm sil} = \frac{3}{4\rho}\left[\frac{(\Delta Q_{HK})_s}{a_s} N_s + \frac{(\Delta Q_{HK})_{\rm IR}}{a_{\rm IR}} N_{\rm IR}\right] \Big/ (N_s + N_{\rm IR}) .$$

The result is $\Delta\xi_{\rm sil} = 0.16 \times 10^4$ cm^2 g^{-1}, for silicate–metal oxide grains.

Substituting for $\Delta\xi_{\rm sil}$ and $\Delta\xi(3.07)$ in

$$\left(\frac{\bar\rho_{\rm ice}}{\bar\rho_{\rm sil}}\right) = \frac{\Delta\xi_{\rm sil}}{\Delta\xi(3.07)}\left[\frac{\Delta m(3.07)}{E_{HK}}\right] ,$$

we find that $(\bar\rho_{\rm ice}/\bar\rho_{\rm sil}) \approx (0.066)[\Delta m(3.07)/E_{HK}]$.

Taking the observations from Table 7 shows that for the less obscured sources showing no significant ice ($E_{HK} \lesssim 2.2$, except for HD 147889) $(\bar\rho_{\rm ice}/\bar\rho_{\rm sil}) \approx 2 \times 10^{-3}$, and for the more heavily obscured sources $(\bar\rho_{\rm ice}/\bar\rho_{\rm sil})$ ranges from 1.7×10^{-2} to 4.4×10^{-2}. As mentioned previously, the silicate–metal oxide model yields a maximum expected value of $(\bar\rho_{\rm ice}/\bar\rho_{\rm sil}) \approx 0.7$. Thus in the less obscured regions of the Ophiuchus cloud the relative ice abundance is $\sim$350 times less than the maximum expected value, and even in the dense regions showing ice, the relative ice abundance is $\sim$30 times less than the maximum expected.

The uncertainties in estimating the relative ice abundance include the facts that other species may contribute to the apparent ice band extinction, that the band strength may depend on the composition of the mixture containing ice, that the ice band complex refractive index is uncertain, that the relative ice abundance must be compared with an uncertain model of the core grain composition and size distribution, and that the conditions and ice abundance vary along the line of sight, tending to cause underestimation of the ice abundance. Considering all of these uncertainties, the uncertainty in the relative ice abundance may be a factor of $\sim$3. Nonetheless, ice seems to be grossly underabundant for densities less than $\sim$5 mag pc^{-1} in E_{HK} and significantly underabundant even for higher densities.

The small ratio of ice mantle mass to core mass suggests the approximation that the mantle volume is the core grain area (area $= 4\sigma_c$, where σ_c is the cross section) times the average mantle thickness (δ). In that case,

$$\frac{\Delta m(3.07)}{E_{HK}} \approx \frac{(2.4 \times 10^4)\rho_{\rm ice}(4\sigma_c\delta)n_g}{\sigma_c \Delta Q_{HK} n_g} .$$

Again using the extinction efficiencies in Table 7, for stars showing measurable ice, $\delta \approx 0.01$ μm—showing that our use of the Rayleigh approximation is quite reasonable.

For such thin mantles, the contribution to the 2 μm extinction from ice, A_K(ice) (where $A_K = E_{K\infty}$), is negligible. If in the near-IR region the absorption is not extreme, then $k \approx 0.01$, the ice refractive index is $m = 1.32 - 0.01i$, and, using the Rayleigh approximation, $[A_K(\text{ice})/\Delta m(3.07)] \approx 0.02$. Comparing with the data in Table 5 and in Table 7, it is apparent that $[A_K(\text{total})/\Delta m(3.07)] \approx 3.5$, and that at most $\sim$1/200 of A_K is due to the presence of ice mantles, even in the most heavily obscured regions. This explains why there is no change in the extinction curves associated with the onset of ice band extinction.

We have been unable to explain completely the rapid onset of ice condensation and the relatively low ice abundance (Harris 1976). A number of points do seem relevant to this question, however.

Cloud density should be important in determining the amount of ice condensation because condensation is a consequence of random encounters between gas atoms and grains. Below the condensation temperature, the standard model predicts $\Delta m(3.07) \propto \int \rho^n ds$, where $n \approx 3$ (Oort and van de Hulst 1946; Greenberg 1968) and ρ is the gas-plus-dust averaged density; while a measure of the continuum extinction such as E_{HK} behaves like $\int \rho ds$.

Both Watson and Salpeter (1972) and Aannestad (1973) give a condensation temperature of $\sim$17 K for ice, whereas the observed dust temperature is $\sim$50 K (Fazio *et al.* 1976). If the dust is heated by starlight through thermally reradiated infrared emission, the denser and more opaque regions would be colder because of self-shielding of this IR radiation, permitting the observed ice condensation. Recently Aannestad (1975) noted that the emissivity of ice in the thermal (at $\sim$50 K) region is larger than that of the expected silicate core particles, suggesting the possibility that once a monolayer of ice forms, the grain cools, causing enhanced condensation. Such a critical process, in combination with self-shielding of IR radiation, might explain the observed dependence of ice abundance on density.

IV. CONCLUSIONS

We have observed the continuum extinction and the 3.07 μm ice band to study the formation of ice mantles on grains in the ρ Oph dark cloud. We have found:

1. The large values of R and $\lambda_{\rm max}$ of polarization in this cloud are not due to the coating of grains with water ice; these anomalies probably result from silicate–metal oxide coating of the grains.

2. Ice band extinction seems to appear abruptly at a critical extinction density of $E_{HK} \approx 5$ mag pc^{-1}. Observations of additional sources, including those in other dark clouds, are needed to test the universality of this relation.

3. There is no significant change in the broad-band extinction with the onset of ice band extinction.

4. Even where ice band extinction is seen, the strength corresponds to only a small fraction of the total amount of ice available, based on solar relative abundances.

We thank P. Aannestad, K. Day, W. K. Hartmann, D. R. Huffman, G. Sill, and S. E. Strom for helpful discussions and the communication of unpublished results. This work was supported by NASA and the National Science Foundation.

REFERENCES

Aannestad, P. A. 1973, *Ap. J. Suppl.*, **25**, 205.
———. 1975, *Ap. J.*, **200**, 30.
Allen, C. W. 1964, *Astrophysical Quantities* (London: Athlone Press).
Appenzeller, I. 1975, *Conf. on Optical Observing Programs on Galactic Structure and Dynamics*, ed. Th. Schmidt-Kaler (Astronomical Institute of Ruhr-University).
Becklin, E. E., and Neugebauer, G. 1968, *Ap. J.*, **151**, 145.
Bertie, J. E., Labbé, H. J., and Whalley, E. 1969, *J. Chem. Phys.*, **50**, 4501.
Blaauw, A. 1963, in *Basic Astronomical Data*, ed. K. Aa. Strand (Chicago: University of Chicago Press), chap. 20.
Brown, R. L., Gammon, R. H., Knapp, G. R., and Balick, B. 1974, *Ap. J.*, **192**, 607.
Carrasco, L., Strom, S. E., and Strom, K. M. 1973, *Ap. J.*, **182**, 95.
Chaldu, R., Honeycutt, R. K., and Penston, M. V. 1973, *Pub. A.S.P.*, **85**, 87.
Fazio, G. G., Wright, E. L., Zeilik, M., and Low, F. J. 1976, *Ap. J.* (*Letters*), **206**, L165.
Frogel, J. A., Persson, S. E., Aaronson, M., Becklin, E. E., Matthews, K., and Neugebauer, G. 1975, *Ap. J.* (*Letters*), **195**, L15.
Garrison, R. F. 1967, *Ap. J.*, **147**, 1003.
Gillett, F. C., Jones, T. W., Merrill, K. M., and Stein, W. A. 1975, *Astr. Ap.*, **45**, 77.
Grasdalen, G. L. 1974, *Ap. J.*, **193**, 373.
Grasdalen, G. L., Joyce, R., Knacke, R. F., Strom, S. E., and Strom, K. M. 1975, *A.J.*, **80**, 117.
Greenberg, J. M. 1966, *Ap. J.*, **145**, 57.
———. 1968, in *Nebulae and Interstellar Matter*, ed. Barbara M. Middlehurst (Chicago: University of Chicago Press), chap. 6.
Greenberg, R., Davis, D. R., Hartmann, W. K., and Chapman, C. R. 1977, *Icarus*, **30**, 769.
Harris, D. H. 1976, Ph.D. thesis, University of Arizona.
Hartmann, W. K. 1976, private communication.
Hiltner, W. A. 1956, *Ap. J. Suppl.*, **2**, 389.
Irvine, W. M., and Pollack, J. B. 1968, *Icarus*, **8**, 324.
Johnson, H. L. 1968, in *Stars and Stellar Systems*, ed. B. Middlehurst and L. H. Aller (Chicago: University of Chicago Press), Vol. **7**, Ch. 5.
Johnson, H. L., Mitchell, R. I., Iriarte, B., and Wisniewski, W. Z. 1966, *Comm. Lunar Planet. Lab.*, **4**, No. 63.
Jones, D. H. P. 1970, *M.N.R.A.S.*, **152**, 231.
King, I. 1952, *A.J.*, **57**, 253.
Knacke, R. F., Cudaback, D. D., and Gaustad, J. E. 1969, *Ap. J.*, **158**, 151.
Knapp, G. R., Kuiper, T. B. H., and Brown, R. L. 1976, *Ap. J.*, **206**, 109.
Martin, P. G., Illing, R., and Angel, J. R. P. 1972, *M.N.R.A.S.*, **159**, 191.
Merrill, K. M., Russell, R. W., and Soifer, B. T. 1976, *Ap. J.*, **207**, 763.
Merrill, K. M., and Soifer, B. T. 1974, *Ap. J.* (*Letters*), **189**, L27.
Merrill, K. M. and Stein, W. A. 1976, *Pub. A.S.P.*, **88**, 285.
Oort, J. H., and van de Hulst, H. C. 1946, *Bull. Astr. Inst. Netherlands*, **10**, 187.
Rydgren, A. E., Strom, S. E., and Strom, K. M. 1976, *Ap. J. Suppl.*, **30**, 307.
Schaaf, J. W., and Williams, D. 1973, *J. Opt. Soc. Am.*, **63**, 726.
Serkowski, K. 1968, *Ap. J.*, **154**, 115.
Shu, F. H. 1975, *La Dynamique des Galaxies Spirales, Colloque Intern*, ed. L. Weliachew, Centre Nat. Res. Sci., No. 241.
Sill, G. 1976, private communication.
Snow, T. P., and Cohen, J. G. 1974, *Ap. J.*, **194**, 313.
Soifer, B. T., Russell, R. W., and Merrill, K. M. 1976, *Ap. J.* (*Letters*), **207**, L83.
Spitzer, L. 1968, *Diffuse Matter in Space* (New York: Wiley).
Strom, S. E., Strom, K. M., and Carrasco, L. 1974, *Pub. A.S.P.*, **86**, 798.
Strom, K. M., Strom, S. E., Carrasco, L., and Vrba, F. J. 1975, *Ap. J.*, **196**, 489.
Strom, K. M., Strom, S. E., and Vrba, F. J. 1976, *A.J.*, **81**, 308.
Strom, S. E., Vrba, F. J., and Strom, K. M. 1976, *A.J.*, **81**, 314.
Struve, O., and Rudkjobing, M. 1949, *Ap. J.*, **109**, 92.
van Breda, I. G., Glass, I. S., and Whittet, D. C. B. 1974, *M.N.R.A.S.*, **168**, 551.
Voelcker, K. 1975, *Astr. Ap. Suppl.*, **22**, 1.
Vrba, F. J., Strom, K. M., Strom, S. E., and Grasdalen, G. L. 1975, *Ap. J.*, **197**, 77.
Walborn, N. R. 1972, *A.J.*, **77**, 312.
Watson, W. D., and Salpeter, E. E. 1972, *Ap. J.*, **175**, 659.
Whittet, D. C. B. 1974, *M.N.R.A.S.*, **168**, 371.
Wickramasinghe, N. C. 1973, *Light Scattering Functions for Small Particles with Applications in Astronomy* (New York: Wiley).
Wilson, R. W., Jefferts, K. B., and Penzias, A. A. 1970, *Ap. J.* (*Letters*), **161**, L43.
Wood, J. A. 1975, in *The Dusty Universe*, ed. G. B. Field and A. G. W. Cameron (New York: Neale Watson), p. 245.
Zellner, B. 1973, *IAU Symposium 52, Interstellar Dust and Related Topics*, ed. J. M. Greenberg and H. C. van de Hulst (Dordrecht: Reidel), p. 109.

D. H. Harris: Project Starlight International, P.O. Box 5310, Austin, TX 78763

G. H. Rieke: Lunar and Planetary Laboratory, University of Arizona, Tucson, AZ 85721

N. J. Woolf: Steward Observatory, University of Arizona, Tucson, AZ 85721